Ultra-compact TE and TM pass polarizers based on vanadium dioxide on silicon

L. Sánchez, S. Lechago, and P. Sanchis*

Nanophotonics Technology Center, Universitat Politècnica de València, Camino de Vera s/n, Valencia 46022, Spain
Corresponding author: pabsanki@ntc.upv.es

Vanadium dioxide (VO_2) is a metal-insulator transition (MIT) oxide recently used in plasmonics, metamaterials, and reconfigurable photonics. Because of the MIT, VO_2 shows great change in its refractive index allowing for ultra-compact devices with low power consumption. We theoretically demonstrate a transverse electric (TE) and a transverse magnetic (TM) pass polarizer with an ultra-compact length of only 1 μm and tunable using the MIT of the VO_2. During the insulating phase, both devices exhibit insertion losses below 2 dB at 1550 nm. Changing to the metallic phase, the unwanted polarization is attenuated above 15 dB while insertion losses are kept below 3 dB. Broadband operation over a range of 60 nm is also achieved.   © 2015 Optical Society of America

OCIS codes: (130.3120) Integrated optics devices; (230.5440) Polarization-selective devices; (230.7370) Waveguides; (160.2100) Electro-optical materials.

http://dx.doi.org/10.1364/OL.40.001452

One of the most crucial topics in optical devices based on silicon photonics is polarization management. Silicon waveguides are highly polarization dependent because of their high index contrast and structural birefringence [1–4]. Transverse electric (TE) and transverse magnetic (TM) modes have a different behavior in the silicon waveguides so a polarization control is necessary to avoid the deterioration of the performance of the devices. Rotators [5–11], converters [12,13], polarization beam splitters [14–19], and polarizers [20–26] have been widely reported in the silicon-on-insulator (SOI) platform. If a polarization division multiplex is not necessary, a common approach consists of using a polarizer to strip off the unwanted polarization [20,23]. To achieve more compact and efficient devices, different polarizers have been proposed, such as using plasmonic waveguides [20–25], photonic crystal slab, and shallowly etched waveguides [26]. A key feature for integrated optical polarizers is to make them externally controlled.

A way to achieve such control can be through the addition to the structure of new materials compatible with CMOS fabrication techniques, with disruptive optical properties. The transition metal oxides have been studied because of their controllable change between an insulator phase and a metallic phase. Vanadium dioxide (VO_2) performs well, showing an abrupt change (several orders of magnitude) in the resistivity and the optical properties between the two phases. This semiconductor-to-metal transition (SMT) is related to a structural transition from a monoclinic to a tetragonal crystal structure. At steady conditions, VO_2 is in the insulator state (high transparence in the infrared spectrum), but its phase can be triggered to a metallic state (absorbing and reflecting properties) by applying an electric field or by optical pumping. Recently, VO_2 has been used for the development of compact switches and modulators [27–37] with low power consumption. Introducing the VO_2 to a polarizer structure makes it possible to control it by the SMT. In this way, the elimination of the unwanted polarization in the polarizer can be controlled by an external signal.

In this work, we have designed tunable hybrids VO_2-silicon polarizers to control the attenuation of the unwanted polarization, taking advantage of the change in the refractive index in the VO_2 during its semiconductor to metal transition. To the best of our knowledge, this is the first time that tunable polarizers compatible with silicon photonics are proposed. Furthermore, devices exhibit an ultra-compact footprint with a total length of only 1 μm, insertion losses below 3 dB, and broadband operation. The schematic diagrams of the proposed TE and TM pass polarizers are shown in Fig. 1.

For the design of the TE pass polarizer, several simulations have been performed using a full-vectorial mode solver based on the finite element method (FEM). A single-mode silicon waveguide with a cross section of 400 × 220 nm shows a TE and a TM mode with a different mode profile. The TE mode has the maximum of its electric field confined in the center of the silicon waveguide. On the other hand, the maximum electric field in the TM mode is concentrated in the horizontal surfaces of the waveguide. Thus, the introduction of a VO_2 film over the waveguide will affect the propagation of the TM modes more than the TE modes. Therefore, by changing
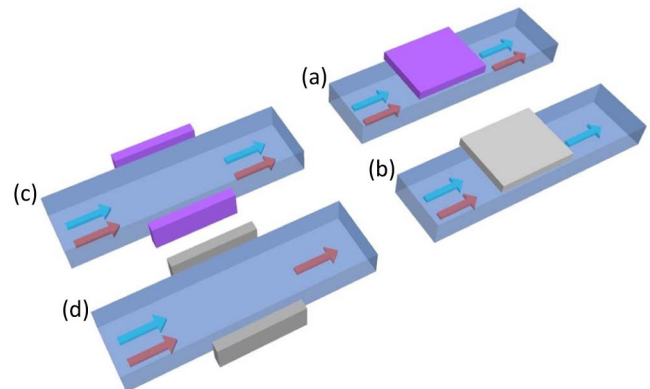

Fig. 1.   Schematics of the (a)–(b) TE and (c)–(d) TM pass polarizers devices. Both structures are surrounded by silica. The blue arrows show TE polarization and the red arrows show TM polarization. The VO_2 in the dielectric state is represented in purple, and the metallic state in the gray.
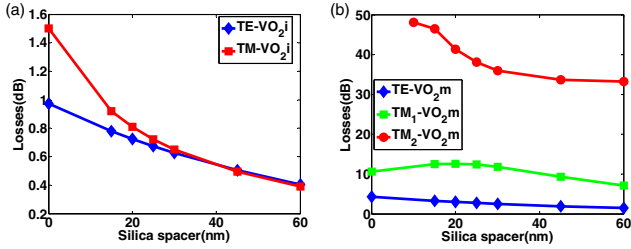
Fig. 2.   (a) Losses for the TE and TM for the insulating state as a function of the silica spacer. (b) Losses for the metallic state as a function of the silica spacer. The waveguide width is set at 400 nm.
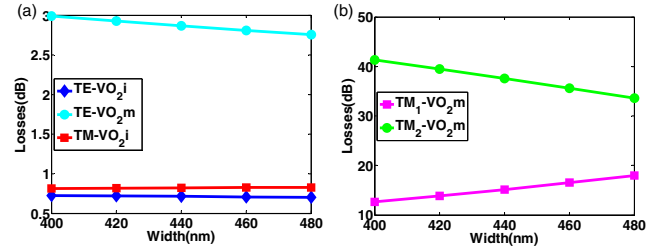

Fig. 3.   Losses as a function of the waveguide width for (a) the TE in both states and the TM in the insulating state and (b) the TM modes in the metallic state. The silica spacer is set at 20 nm.

the VO_2 phase, it is possible to control the rejection of the TM polarization.

To achieve an active TE pass polarizer with good performance, in the insulating state both polarizations should pass through the polarizer with low losses. On the other hand, in the metallic state, the TE polarization should have low losses while the TM polarization should have high losses.

The design of the polarizer starts with a waveguide with a cross section of 400×220 nm with a VO_2 film on top with a length of 1 μm and a thickness of 70 nm. The VO_2 refractive index [29] is $3.21 + 0.17i$ and $2.15 + 2.79i$ for the insulating and the metallic states, respectively. The first parameter under study is the silica spacer between the waveguide and the VO_2. Figure 2 shows the losses for the TE and TM polarizations as a function of the VO_2 phase and the silica spacer thickness at 1550 nm.

In an insulating state, if the spacer is thinner, the losses are higher because the modes have a stronger interaction with the VO_2 film. In Fig. 2(a), increasing the spacer is related to a reduction of losses because of the lower interaction. In any case, for a spacer higher than 15 nm, the losses for both polarizations are lower than 1 dB. On the other hand, in the metallic state, for a spacer higher than 10 nm, it should be noticed that a second TM mode appears but with a high level of losses. If the input field excites both TM modes, it will provide an extra level of losses so it will improve the performance. As was mentioned before, in this state, the polarizer should have low losses in TE and high losses in TM. Taking into account this trade-off, for a silica spacer of 20 nm, the TM shows a local maximum of 12.5 dB while the losses in TE are below 3 dB. Once the silica spacer has been optimized to 20 nm, the width of the waveguide has also been optimized. The restriction in this case is the single-mode condition in the insulating state. Studying the structure, the maximum width that ensures the single-mode condition in the insulating state is 480 nm. Figure 3 shows the losses as a function of waveguide width using a silica spacer of 20 nm for TE and TM in both states.

For the TE polarization, Fig. 3(a), it is desirable to achieve the lowest losses as possible for both states. Increasing the width of the waveguide, the losses decrease slightly so higher widths are more appropriate. In the insulating state, the losses for TM polarization are also maintained below 1 dB. On the other hand, it can be seen in Fig. 3(b) that higher widths also contribute to an increase in the losses of the first TM mode in the metallic state which will determine the total attenuation of the unwanted polarization. Again, it is interesting to note that higher widths are required for appropriate performance of the polarizer. In this way, with a silica spacer of 20 nm and a width of 480 nm the losses for TE and TM in insulating state are 0.7 and 0.8 dB, while the losses in the metallic state are 2.8 dB and above 15 dB, respectively.

To confirm the results, the structure has been simulated using a three-dimensional finite integration technique (FIT) which solves Maxwell equations using the recurrent integral method and a hexahedral mesh.

Figures 4(a) and 4(b) show the performance of the device for both polarizations when the VO_2 is in the insulating state. In both cases, the field goes through the device with low attenuation. On the other hand, Figs. 4(c) and 4(d) describe the performance in the metallic state. It can be seen that the attenuation for TM is very high and the signal is almost eliminated. The performance of the device has also been studied for a range of wavelengths of 100 nm. In this case, three-dimensional finite difference time-domain (FDTD) simulations were performed. Figure 5 shows the spectral response for (a) TE and (b) TM polarizations. It can be seen that results are in good agreement with the ones calculated by analyzing the modes which indicates that coupling losses, as well as the effect of the finite length of the
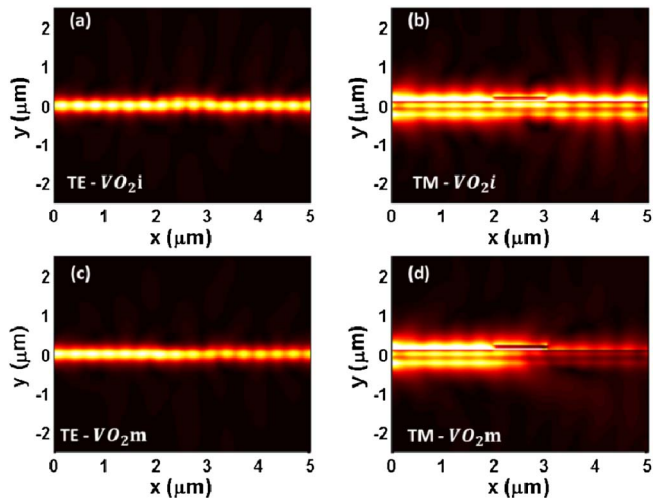

Fig. 4.   TE pass polarizer performance for the different light polarizations and VO_2 states. Lateral view of the device. TE and TM polarizations for the (a)–(b) insulating and (c)–(d) the metallic states.
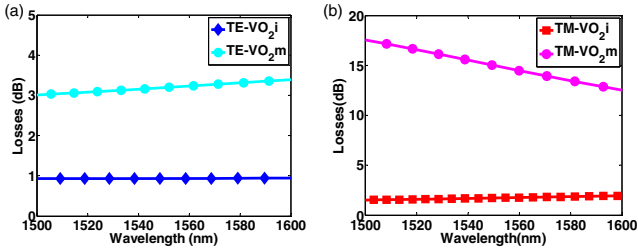
Fig. 5. Transmission of TE and TM polarization as a function of the wavelength and the VO_2 state for the TE pass polarizer.

Fig. 7. Transmission of the TM pass polarizer as a function of the silica spacer for both light polarizations and VO_2 states. The waveguide width is set at 300 nm.

structure, are almost negligible. The losses for TE polarization in the metallic state are slightly higher than 3 dB when the wavelength increases. On the other hand, the extinction ratio of the TM in the metallic state also decreases when the wavelength is increased, but the attenuation is always higher than 12.5 dB for the whole wavelength range.

For the active TM pass polarizer, to achieve a high interaction between the VO_2 and the TE mode, the VO_2 film must be on the sides of the waveguide. To achieve a higher interaction, the width of the waveguide must be decreased to delocalize the mode. At the same time, the width must be high enough to ensure low propagation losses. Our trade-off consists of achieving the maximum attenuation of the unwanted TE polarization in the metallic state by keeping insertion losses below 3 dB. The influence of the waveguide width and the thickness of the silica spacer between the silicon waveguide and the VO_2 also have analyzed. Fixing the silica spacer to 20 nm, the width of the waveguide has been decreased from 400 to 300 nm.

In Fig. 6(a), it can be seen that insertion losses are slightly increased when the waveguide width decreases. However, narrower waveguides allow a significant increase in the attenuation of the TE polarization in the metallic state, as it is depicted in Fig. 6(b). Therefore, an optimum width of 300 nm has been chosen to ensure that insertion losses are below 3 dB at both VO_2 states. Once the optimum width has been selected, the influence of the silica spacer has also been analyzed. Results are shown in Fig. 7. Smaller spacers also contribute an increase in insertion losses, as seen in Fig. 7(a); on the other hand, they have the benefit of a larger attenuation of the unwanted TE polarization, as shown in Fig. 7(b). Therefore, a silica spacer width of 10 nm has been chosen to keep insertion losses below 3 dB.

Figure 8 shows the performance of the TM polarizer for the different states and polarizations. For the
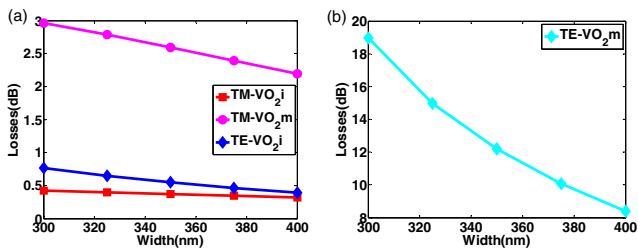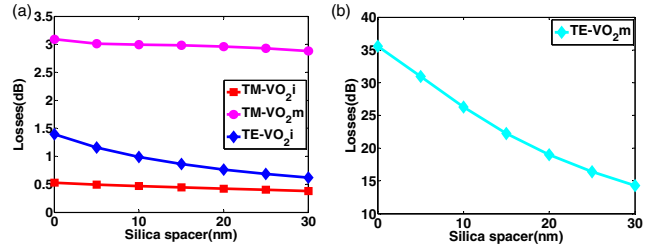
insulating state, Figs. 8(a) and 8(b), the optical field shows a low attenuation for both polarizations while, for the metallic state, the field is highly attenuated for the TE polarization [Fig. 8(c)] and low attenuated for TM polarization [Fig. 8(d)].

In Fig. 9, the spectral response calculated with a three-dimensional FDTD is shown to be between 1500 and 1600 nm. It can be seen that a broadband operation range is also achieved.

Results are also in good agreement with those calculated by analyzing the modes, except for the extinction ratio, of the unwanted TE polarization. The attenuation was higher than 20 dB in Fig. 7(b). However, by using the FDTD as well as FIT simulations, the attenuation is reduced to around 17 dB at 1550 nm. We attribute this discrepancy to the finite length of the structure. In any case, the attenuation is above 12.5 dB for the whole wavelength range.

To achieve full control of the polarization of the input signal, the two proposed polarizers can be integrated in a compact structure to control both polarizations. Figure 10 shows the schematic of the combined structure. The tapers of 3 μm length have also been simulated to ensure negligible losses during the transitions between waveguides with different cross sections. The total footprint of the device would be lower than 4 μm². Depending on which polarizer is active, it is possible to eliminate the unwanted polarization. Three main cases must be
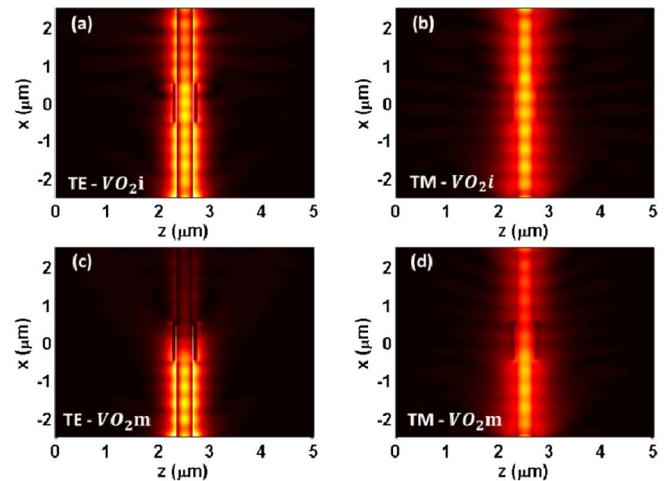

Fig. 6. Transmission of the TM pass polarizer as a function of the waveguide width for both light polarizations and VO_2 states. The silica spacer is 20 nm.

Fig. 8. TM pass polarizer performance for the different light polarizations and VO_2 states. Top view of the device. TE and TM polarizations for the (a)–(b) insulating and (c)–(d) metallic states.
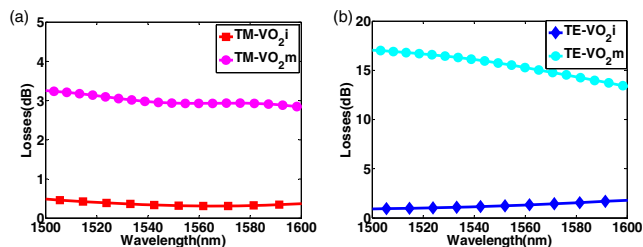
Fig. 9. Transmission of TE and TM polarization as a function of the wavelength and the VO_2 state for the active TM pass polarizer.
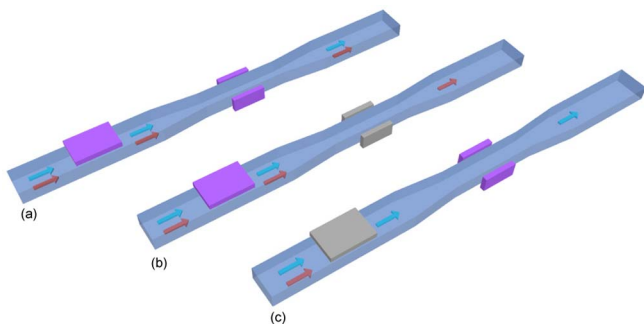

Fig. 10. Schematic of the combined structure for the three main performance modes. The VO_2 in insulating state is represented in purple, and the metallic state in gray color.

considered: both polarizers in the insulating state and TM pass polarizer, and the TE pass polarizer in the metallic state [Figs. 10(a)–10(c), respectively]. For the first case, both polarizations would show losses below 3 dB and, in the other cases, the unwanted polarization would be attenuated above 17 dB while the desired polarization would have losses below 5 dB.

In summary, the design of tunable TE and TM pass polarizers based on a hybrid VO_2/Si waveguide structure has been described. Tunability is achieved by exploiting the ultra large change of the refractive index in the VO_2 between the insulating and the metallic states. Both polarizers can be combined to achieve an ultra-compact structure which would allow complete polarization management. The integration of VO_2 with silicon is a promising approach for pushing forward the limits of the current silicon technology.

References

1. R. Soref and J. Lorenzo, IEEE J. Quantum Electron. **22**, 873 (1986).
2. B. Jalali and S. Fathpour, J. Lightwave Technol. **24**, 4600 (2006).
3. C. Manolatou, S. G. Johnson, S. Fan, P. R. Villeneuve, H. A. Haus, and J. D. Joannopoulos, J. Lightwave Technol. **17**, 1682 (1999).
4. L. Chen, C. R. Doerr, and Y. Chen, in *Optical Fiber Communication Conference* (Optical Society of America, 2012), paper OW3G.7.
5. C. A. Ramos, R. Halir, A. O. Moñux, P. Cheben, L. Vivien, I. M. Fernández, D. M. Morini, S. Janz, D. X. Xu, and J. Schmid, Opt. Lett. **37**, 3534 (2012).
6. H. Zhang, S. Das, Y. Huang, C. Li, and S. Chen, Appl. Phys. Lett. **101**, 021105 (2012).
7. M. Aamer, A. M. Gutierrez, A. Brimont, D. Vermeulen, G. Roelkens, J. M. Fedeli, A. Håkansson, and P. Sanchis, IEEE Photon. Technol. Lett. **24**, 2031 (2012).
8. M. Komatsu, K. Saitoh, and M. Koshiba, IEEE Photon. J. **4**, 707 (2012).
9. J. N. Caspers, M. Z. Alam, and M. Mojahedi, Opt. Lett. **37**, 4615 (2012).
10. G. Chen, L. Chen, W. Ding, F. Sun, and R. Feng, Opt. Lett. **38**, 1984 (2013).
11. L. Gao, Y. Huo, J. S. Harris, and Z. Zhou, in *IEEE 10th International Conference on Group IV* (IEEE, 2013), pp. 43–44.
12. K. Nakayama, Y. Shoji, and T. Mizumoto, IEEE Photon. Technol. Lett. **24**, 1310 (2012).
13. L. Sánchez and P. Sanchis, Opt. Lett. **38**, 2842 (2013).
14. H. Zhan, Y. Huang, S. Das, C. Li, M. Yu, P. G. Q. Lo, M. Hong, and J. Thong, Opt. Express **21**, 3363 (2013).
15. Y. Ding, L. Liu, C. Peucheret, and H. Ou, Opt. Express **20**, 20021 (2012).
16. Y. Ding, H. Ou, and C. Peucheret, Opt. Lett. **38**, 1227 (2013).
17. D. Dai and J. E. Bowers, Opt. Express **19**, 10940 (2011).
18. Z. Xiao, X. Luo, P. H. Lim, P. Prabhathan, S. T. H. Silalahi, T. Y. Liow, J. Zhang, and F. Luan, Opt. Express **21**, 16331 (2013).
19. J. Chee, S. Zhu, and G. Q. Lo, Opt. Express **20**, 25345 (2012).
20. Y. Huang, S. Zhu, H. Zhang, T. Y. Liow, and G. Q. Lo, Opt. Express **21**, 12790 (2013).
21. X. Sun, M. Z. Alam, S. J. Wagner, J. S. Aitchison, and M. Mojahedi, Opt. Lett. **37**, 4814 (2012).
22. M. Alam, J. S. Aitchsion, and M. Mojahedi, Appl. Opt. **50**, 2294 (2011).
23. M. Z. Alam, J. S. Aitchison, and M. Mojahedi, Opt. Lett. **37**, 55 (2012).
24. Z. Ying, G. Wang, X. Zhang, Y. Huang, H. P. Ho, and Y. Zhang, IEEE Photon. Technol. Lett. **27**, 201 (2015).
25. I. Avrutsky, IEEE J. Sel. Top. Quantum Electron. **14**, 1509 (2008).
26. D. Dai, Z. Wang, N. Julian, and J. E. Bowers, Opt. Express **18**, 27404 (2010).
27. J. D. Ryckman, V. D. Blanco, J. Nag, R. E. Marvel, B. K. Choi, R. E. Haglund, and S. M. Weiss, Opt. Express **20**, 13215 (2012).
28. D. Ruzmetov, G. Gopalakrishnan, C. Ko, V. Narayanamurti, and S. Ramanathan, J. Appl. Phys. **107**, 114516 (2010).
29. R. M. Briggs, I. M. Pryce, and H. A. Atwater, Opt. Express **18**, 11192 (2010).
30. B. A. Kruger, A. Joushaghani, and J. K. S. Poon, Opt. Express **20**, 23598 (2012).
31. K. J. A. Ooi, H. S. Chu, and L. K. Ang, Nanophotonics **2**, 13 (2013).
32. S. Chen, X. Yi, H. Ma, H. Wang, X. Tao, M. Chen, and C. Ke, Opt. Quantum Electron. **35**, 1351 (2003).
33. P. Markov, J. D. Ryckman, R. E. Marvel, K. A. Hallman, R. F. Haglund, and S. M. Weiss, in *Conference on Lasers and Electro-Optics* (Optical Society of America, 2013), paper CTu2F.7.
34. A. Joushaghani, B. A. Kruger, S. Paradis, D. Alain, J. S. Aitchison, and J. K. S. Poon, Appl. Phys. Lett. **102**, 061101 (2013).
35. J. D. Ryckman, K. A. Hallman, R. E. Marvel, R. F. Haglund, and S. M. Weiss, Opt. Express **21**, 10753 (2013).
36. L. A. Sweatlock and K. Diest, Opt. Express **20**, 8700 (2012).
37. J. T. Kim, Opt. Lett. **39**, 3997 (2014).